



Confinement of superconducting fluctuations due to emergent electronic inhomogeneities

C. Carbillet,¹ S. Caprara,^{2,3} M. Grilli,^{2,3} C. Brun,¹ T. Cren,¹ F. Debontridder,¹ B. Vignolle,⁴ W. Tabis,^{4,5} D. Demaille,¹ L. Largeau,⁶ K. Ilin,⁷ M. Siegel,⁷ D. Roditchev,^{1,8} and B. Leridon^{8,*}

¹*Institut des Nanosciences de Paris, Sorbonne Universités-UPMC-CNRS, F-75005 Paris, France*

²*Department of Physics, Università La Sapienza, Piazzale A. Moro 5, I-00185 Rome, Italy*

³*ISC-CNR, via dei Taurini 19, I-00185 Rome, Italy*

⁴*Laboratoire National des Champs Magnétiques Intenses, CNRS-INSA-UJF-UPS, F-31400 Toulouse, France*

⁵*AGH University of Science and Technology, Faculty of Physics and Applied Computer Science, Aleja Mickiewicza 30, PL-30-059 Krakow, Poland*

⁶*Laboratoire de Photonique et Nanostructures, CNRS, Route de Nozay, F-91460 Marcoussis, France*

⁷*Institute of Micro- und Nano-electronic Systems, Karlsruhe Institute of Technology, Hertzstrasse 16, D-76187 Karlsruhe, Germany*

⁸*LPEM, ESPCI Paris-PSL Research University-CNRS-Sorbonne Universités, UPMC, F-75005 Paris, France*

(Received 25 November 2015; revised manuscript received 17 March 2016; published 15 April 2016)

The microscopic nature of an insulating state in the vicinity of a superconducting state in the presence of disorder is a hotly debated question. While the simplest scenario proposes that Coulomb interactions destroy the Cooper pairs at the transition, leading to localization of single electrons, an alternate possibility supported by experimental observations suggests that Cooper pairs instead directly localize. The question of the homogeneity, granularity, or possibly glassiness of the material on the verge of this transition is intimately related to this fundamental issue. Here, by combining macroscopic and nanoscale studies of superconducting ultrathin NbN films, we reveal nanoscale inhomogeneities that emerge when the film thickness is reduced. For the thinnest films, scanning tunneling spectroscopy at low temperature unveils inhomogeneities in the superconducting properties, of typical size L_i , that are not correlated to any structural inhomogeneity and that are found to persist above the critical temperature in the form of a pseudogap. Remarkably enough, while the thickest films display a purely two-dimensional behavior in the superconducting fluctuations above the critical temperature, paraconductivity in the pseudogap regime of the thinnest samples demonstrates fluctuations of the amplitude of the order parameter, corresponding to zero-dimensional fluctuating regions of size precisely L_i . We propose that an anomalous diffusion slowing-down process is at play at long wave vectors, leading to some “confinement” of the superconducting fluctuations, which allows us to explain the simultaneous paradoxical presence of a pseudogap and zero-dimensional amplitude fluctuations of the order parameter. These findings call for further theoretical investigation to understand this intermediate state where Cooper pairs continuously evolve from a bound state of fermionic objects into localized bosonic entities.

DOI: [10.1103/PhysRevB.93.144509](https://doi.org/10.1103/PhysRevB.93.144509)

I. INTRODUCTION

Understanding the microscopic processes occurring at the superconductor-insulator transition (SIT) in ultrathin films is important not only for fundamental reasons but also for applicative purposes [1,2]. The microstructural properties are known to play a key role, and the samples can then be divided into two groups [3]: granular thin films and homogeneously disordered thin films. For the former, the SIT is driven by the competition between the intergrain Josephson coupling, favoring the delocalization of pairs, and the Coulomb charging energy of the grains, which renders charge fluctuations energetically expensive [4]. However, in the case of nominally homogeneously disordered films, which are the object of this paper, several scenarios have been proposed.

On the one hand, what is often referred to as the “fermionic” scenario proposes that the mechanism that drives the transition is the reduced screening of the Coulomb repulsion with increasing disorder, weakening pairing, and reducing the critical temperature T_c [5], as observed in [6]. In this case, the insulating state is composed of localized fermions, and

in particular, conventional paraconductive fluctuations are expected due to Gaussian-distributed short-lived Cooper pairs.

On the other hand, pairs may survive the SIT in a “bosonic” scenario, in which the gap persists above T_c despite the loss of phase coherence. In this framework, either the bosonic pairs localize because disorder-enhanced Coulomb interactions destroy their phase-coherent motion at large scales [7,8], or disorder itself can blur the pair phase coherence without any relevant role of the Coulomb repulsion [9–12]. On the experimental side, it has been shown through careful study of Little-Parks oscillations that either fermionic [13] or bosonic [14,15] transitions may occur. In the latter case, it was also proposed that the superconducting state is characterized by an emergent disordered glassy phase [12] with filamentary superconducting currents [9]. An anomalous distribution of the superconducting order parameter was proposed by theorists [12,16,17] and observed experimentally [18,19]. A numerical approach to uniformly disordered superconductors [20] has also suggested that there is a continuous evolution [21] from the weak disorder limit, where the system has a rather homogeneous fermionic character, to the strong disorder limit, where marked inhomogeneities appear in the superconducting order parameter, with an emergent bosonic nature characterized by a single-particle gap persisting on the insulating side. A great

*Corresponding author: brigitte.leridon@espci.fr

deal of experimental activity has been devoted to the more disordered part of the SIT [18,22], while the intermediate region where fermionic Cooper pairs begin to evolve into bosonic pairs has not been as extensively investigated.

The aim of this work is precisely to fill this gap by reporting experiments which shed light on how Cooper pairs evolve with increasing disorder, giving rise to incipient inhomogeneous bosonic features. More specifically, we present in this paper a study on a set of ultrathin NbN films that are nominally homogeneous, but in which electronic inhomogeneities and pseudogap emerge as the thickness is reduced, together with experimental indications in favor of fermionic mechanisms.

Indeed, while the thickest films ($d > 2.2$ nm, $T_c \geq 0.3 T_c^{\text{bulk}} \sim 5$ K) are found to be rather homogeneous [23] with two-dimensional (2D) Aslamazov-Larkin (AL) superconducting fluctuations, the thinnest samples offer a more complex behavior characterized by inhomogeneous superconductivity, by indication of a pseudogap above T_c (a seemingly “bosonic” feature), in agreement with the literature [18,19,24], and by the establishment of a regime of Gaussian superconducting fluctuations (a fermionlike hallmark). In addition, we show that for the “thinnest” films, or, more precisely, films for which the critical temperature is below a certain threshold $T_c \lesssim 0.3 T_c^{\text{bulk}}$, the superconducting fluctuations measured by transport above T_c behave in agreement with a formal *zero-dimensional* (0D) limit of the AL theory of paraconductivity, in a substantial range of reduced temperature $\epsilon \equiv \ln(T/T_c)$. This indicates that these fluctuations are still conventional and consistent with BCS theory but somehow confined in a “supergrain” over a length scale l_{sg} .

On the other hand, the superconducting inhomogeneities as evidenced by scanning tunneling spectroscopy at low temperature correspond to electronic domains of typical size $L_i/2$ precisely of the order of $l_{sg} \sim 50$ nm, i.e., much larger than any definite structural scale of the system.

The paradoxical presence of 0D AL fluctuations together with indications for bosonic features such as the pseudogap, well established in these systems [18,19,24], is one of the most intriguing results of this work. We suggest that these two features can indeed be reconciled if the pseudogap in our system has a fluctuational origin [25]. We also propose that the amplitude of the pseudogap observed in the films under investigation arises from a diffusion slowdown of the fluctuating Cooper pairs, which exhibit a tendency to localize, or, more precisely, *to be confined*, on the typical scale $L_i/2$ and which, simultaneously, give rise to the 0D AL behavior.

II. EXPERIMENTS

Our samples consist of ultrathin NbN films grown *ex situ* on sapphire substrates. Details of the fabrication process may be found in [26] (see also the Supplemental Material [27]). The different samples studied together with their thickness, critical temperature, and resistance per square at room temperature may be found in Table 1 of the Supplemental Material.

Transmission electron microscopy (TEM) measurements of our NbN films (see Fig. 1 in the Supplemental Material) were able to show that the films are smooth and well crystallized and can be viewed as a closely packed assembly of nanocrystallites

of different orientations. These contiguous nanocrystals have typical lateral dimensions d_g of about 2–5 nm.

A. Probing the inhomogeneities with STM and STS

This characteristic film structure is also reflected in topographic scanning tunneling microscopy (STM) images, such as the one presented in Fig. 1(a) for a nominally 2.14-nm-thick sample X_0 ($T_c = 3.8$ K). T_c in this case is measured *in situ* by transport. The film surface is very flat, and the observed nanoscale structures correlate well with the nanocrystals revealed by TEM. At the same time the landscape of the sample also displays smooth inhomogeneities on a larger scale of a few tens of nanometers.

In order to get insight into the superconducting (in)homogeneity of these ultrathin films, we performed scanning tunneling spectroscopy (STS) experiments. In Fig. 1(b) we report the extracted superconducting gap map $\Delta(X, Y)$ at 300 mK, i.e., well inside the superconducting state for the area corresponding to the topographic map of Fig. 1(a). $\Delta(X, Y)$ is defined from the dI/dV spectra as the peak-to-peak energy [see Fig. 2(a) for the corresponding representative dI/dV spectra]. In agreement with previous measurements in similar systems [18,22], we observe spatial variations of the gap [see Fig. 1(b)] and of the integrated in-gap conductance [see Fig. 2(c)]. However, we observe here that *these gap variations are not correlated to the topography of the surface*. Indeed, the cross-correlation map between the maps in Figs. 1(a) and 1(b), displayed in Fig. 1(c), reveals the absence of correlation.

In Fig. 1(d) we report the autocorrelation map of the gap map shown in Fig. 1(b). It allows us to extract both the typical size of domains of constant gap values, hereafter called supergrains, and the typical distance L_i between the centers of such adjacent supergrains. The radial profile extracted from the center of the autocorrelation map is shown in Fig. 1(f), featuring a correlation length L_i of about 100 nm and a typical domain size of about $L_i/2$. This is more than ten times larger than the size of the microstructural grains $d_g \simeq 2\text{--}5$ nm [see Fig. 1(e), depicting the relevant lengths scales].

We present in Figs. 2(a) and 2(b) the representative $dI/dV(V)$ tunneling spectra measured at 300 mK and 4.2 K in the area of interest shown in Fig. 1(a). The blue spectra correspond to the lower gap areas (blue areas) of the gap map presented in Fig. 1(b), while the red spectra are typical of the larger gap areas (red areas) of Fig. 1(b). As may be seen in Fig. 2(b), a spatially varying pseudogap between about -1 and $+1$ mV is observed at 4.2 K, with the characteristic energy scale of the superconducting gap measured at 300 mK. Please note that at 4.2 K all coherence peaks have disappeared, discarding the possibility of a locally higher $T_c > T$.

In order to establish the presence of this pseudogap, we have performed an analysis of the Altshuler-Aronov background [28] by acquiring some tunneling spectra at higher energy (up to 30 meV). We found that the deepest Altshuler-Aronov backgrounds are associated with the smallest superconducting gaps. (The flattest Altshuler-Aronov backgrounds are therefore associated with the largest superconducting gaps.) On the contrary, the strongest dips observed at the zero energy in the 4.2 K conductance map [Fig. 2(b)] are observed in the regions with the highest superconducting gaps

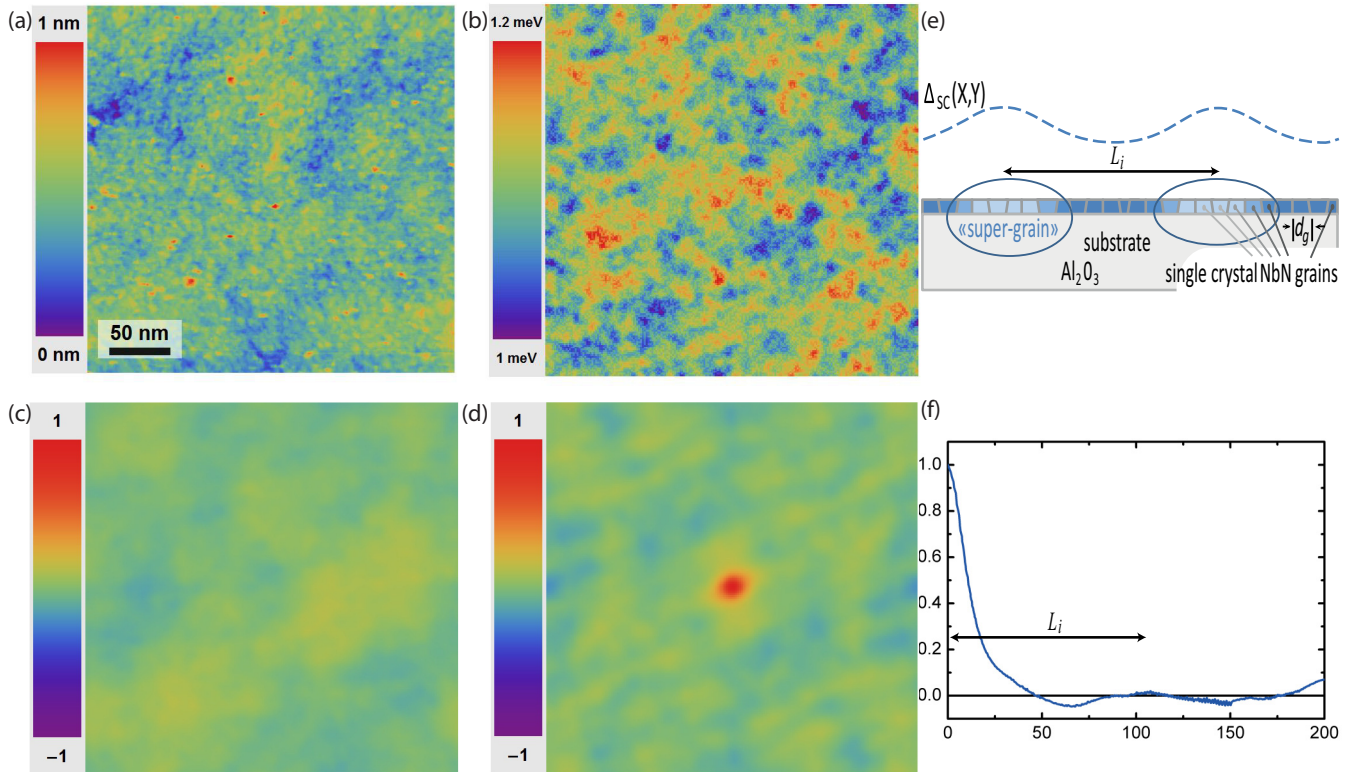


FIG. 1. Local inhomogeneities of the superconducting state. (a) Topographic map of the NbN area under study for sample X_0 ($T_c = 3.8$ K). (b) Corresponding map displaying the superconducting gap inhomogeneities at 300 mK. Gap inhomogeneities appear on a much larger scale than the size of the nanocrystals ($d_g \sim 2\text{--}5$ nm) constituting the NbN films and seen in the topographic map. (c) Cross-correlation map between the topographic and spectroscopic maps revealing the absence of correlation. (d) Autocorrelation map of the gap map in (b). (e) Schematics of the relevant length scales. (f) Radial profile extracted from the autocorrelation map in (d). The correlation length L_i is defined as the abscissa of the first peak away from the center and so is about 100 nm in the present sample. The central peak width, about $L_i/2 \sim 50$ nm, gives an estimate of the typical domain size.

measured at 300 mK. Thus the dips observed at low energy are anticorrelated with the value of the Altshuler-Aronov background, which proves that the dip observed between -1 and $+1$ mV cannot be ascribed to the background. Moreover, in another set of experiments, we observed that when the temperature is increased above 8–10 K, the low zero-bias conductance regions associated with this dip disappear, as expected for a phenomenon related to superconducting correlations. A similar behavior was observed by increasing the magnetic field at 300 mK, 2 K, and 4 K [29].

Figures 2(c) and 2(d) display the dI/dV conductance maps integrated in the energy range of the low-temperature superconducting gaps at 300 mK and at 4.2 K, respectively. It is clear from Fig. 2(d) that some superconducting correlations and superconducting inhomogeneities persist above T_c . In addition, our analysis shows that these two conductance maps in Figs. 2(c) and 2(d) measured over the same topographic area are strongly correlated. This result can be seen in Fig. 2(e), where the cross-correlation map between Figs. 2(c) and 2(d) is plotted. This proves that the spatial inhomogeneities in the energy gap value below T_c and in the pseudogap features above T_c are strongly correlated. Furthermore, the radial profile shown in Fig. 2(f), extracted from a circular average of the cross-correlation map in Fig. 2(e), allows us to infer that the characteristic correlation length of these inhomogeneities at

4.2 K is comparable to the one seen at 300 mK, with size $L_i \sim 100$ nm. We have also performed STS measurements on sample X_0 at higher temperature well into the 0D regime (around 7 K), which show results similar to the one presented in Figs. 2(b) and 2(d) at 4.2 K. The only difference between the 7 and 4.2 K data is that the spectroscopic features related to the pseudogap are smaller in amplitude at 7 K. But the regions where the pseudogap is still present (corresponding to the supergrains) have the same characteristic spacing as at 300 mK, 4.2 K, or even 7 K.

It is noteworthy that the critical temperature measured by *in situ* transport coincides with the temperature of the disappearance of the coherence peaks in the STS spectra. Taking the value of the superconducting gap from the same spectra, the $2\Delta/T_c$ factor is found to be much higher than the bulk NbN value. This was previously observed in [18,19,24].

Therefore, we have shown that some inhomogeneity in the superconductive properties (below and above T_c) emerges for the thinner samples over a scale L_i , while the structural inhomogeneity scale is an order of magnitude smaller. (This result is qualitatively consistent with predictions from Monte Carlo simulations [20].) By contrast, similar spectroscopic studies carried out on thicker samples ($d \geq 2.3$ nm, $T_c \geq 0.3 T_c^{\text{bulk}}$) revealed a much more homogeneous superconducting phase [23].

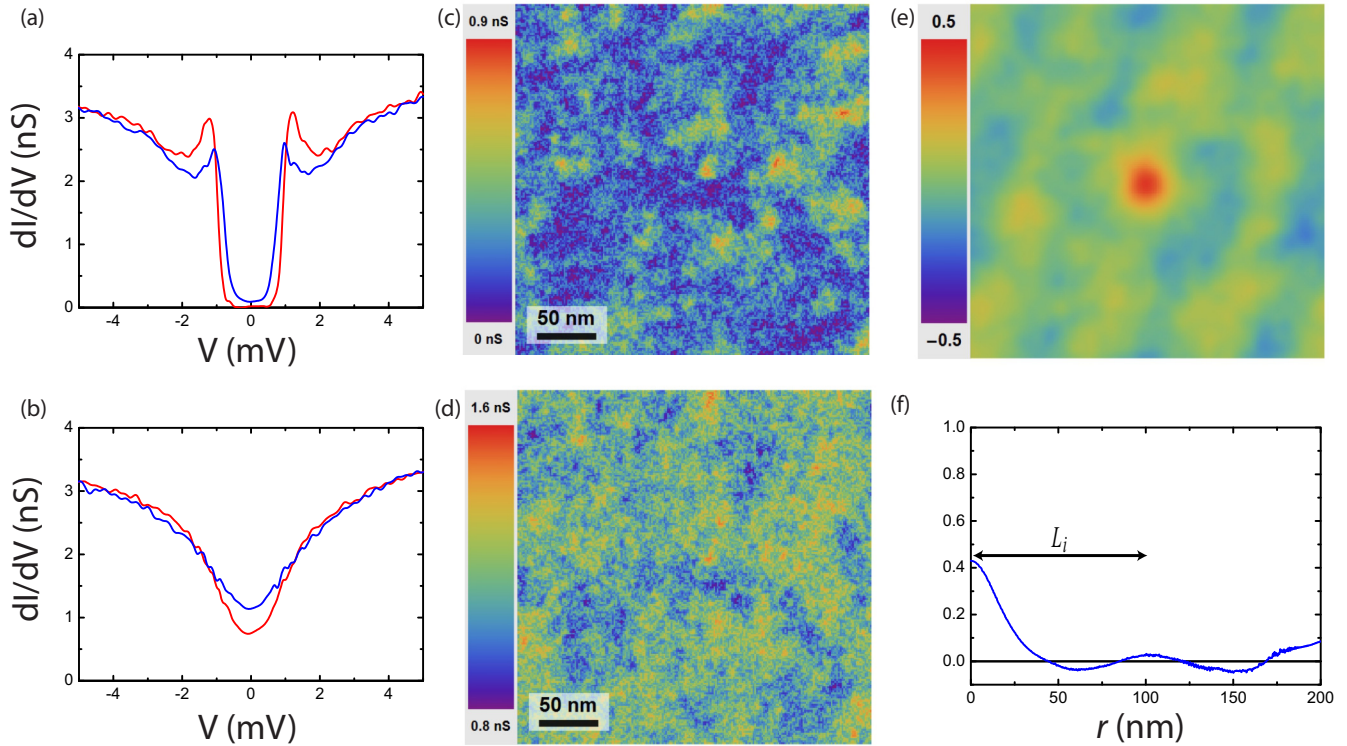


FIG. 2. dI/dV tunneling conductance spectra as a function of bias voltage measured by STS on sample X_0 at (a) 300 mK and (b) 4.2 K. A spatially varying pseudogap is measured at 4.2 K, having the characteristic energy scale of the superconducting gap. The blue spectra are measured on the lower gap areas (blue areas) of the gap map shown in Fig. 1(b), while red spectra are measured on larger gap areas of Fig. 1(b). (c) dI/dV conductance map integrated in the energy range ± 0.9 meV (inside the low-temperature energy-gap region) at 300 mK. The observed inhomogeneities correspond to those seen in the gap map of the main text shown in Fig. 1(b). (d) Same quantity as in (c) but at 4.2 K. This map evidences inhomogeneities above T_c in the pseudogap features. (e) Cross-correlation map between (c) and (d) showing that the inhomogeneities at 300 mK and at 4.2 K are strongly correlated. (f) Radial profile extracted from the cross-correlation map in (e). This analysis allows us to conclude that the length scale L_i characteristic of the superconducting inhomogeneities is the same at 300 mK and at 4.2 K.

B. Paraconductivity measurements

In order to probe the influence of these nanoscale inhomogeneities on the superconducting thermal fluctuations, we performed transport measurements in the vicinity of T_c and extracted the paraconductance per square $\Delta\sigma(T) = \sigma(T) - \sigma_N(T)$, i.e., the excess conductance per square due to superconducting fluctuations in the normal state. Here, $\sigma(T)$ is the square conductance measured under zero magnetic field, and $\sigma_N(T)$ is the normal-state square conductance. The resistance per square is displayed in Fig. 3 for the different samples, together with the extrapolated [Fig. 3(a), solid lines] or measured [Fig. 3(b), solid symbols] resistance of the normal state. (See the methods section in the Supplemental Material for details on the determination of the normal-state resistance.)

In Fig. 4(a) the variation of $\Delta\sigma$ with the reduced temperature $\epsilon \equiv \ln(T/T_c)$ is shown for samples B_2, C_1 , and F_0 : the observed critical exponent -1 is consistent with the Aslamasov-Larkin prediction for 2D systems (AL 2D) [30] $\Delta\sigma = e^2/(16\hbar\epsilon)$ in the range $0.02 \leq \epsilon \leq 0.2-0.9$, as was reported previously for these films [26]. Remarkably, the extracted experimental AL 2D prefactor matches the theoretical one, without any adjustable parameter. This suggests that the fluctuations in this case are BCS-like and that Maki-Thomson (MT) fluctuations [31,32] or density-of-state (DOS) corrections [4,33,34] are absent or negligible.

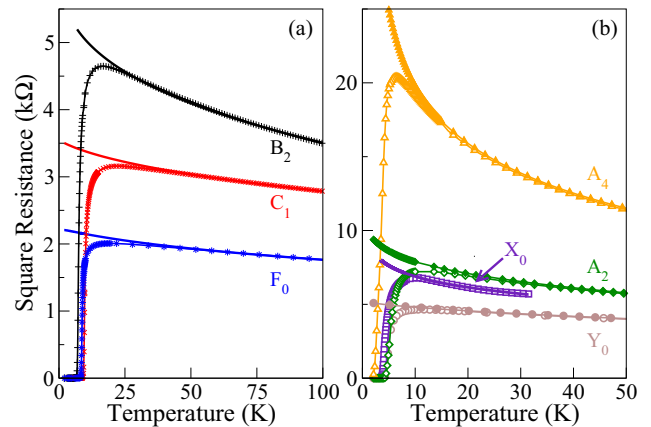


FIG. 3. (a) Square resistance under 0 T as a function of temperature for the thicker samples B_2 ($T_c = 7.1$ K, pluses), C_1 ($T_c = 9.4$ K, crosses), and F_0 ($T_c = 9.0$ K, asterisks), with the corresponding extrapolated normal-state resistance (solid lines; see text). (b) Square resistance under 0 T as a function of temperature for the thinner samples Y_0 ($T_c = 4.3$ K, open circles), X_0 ($T_c = 3.8$ K, open squares), A_2 ($T_c = 4.5$ K, open diamonds), and A_4 (aged A_2 , $T_c = 2.4$ K, open triangles). The square resistances under a perpendicular magnetic field of 14 T are reported with the corresponding solid symbols. The solid lines are for the extrapolated normal-state resistances.

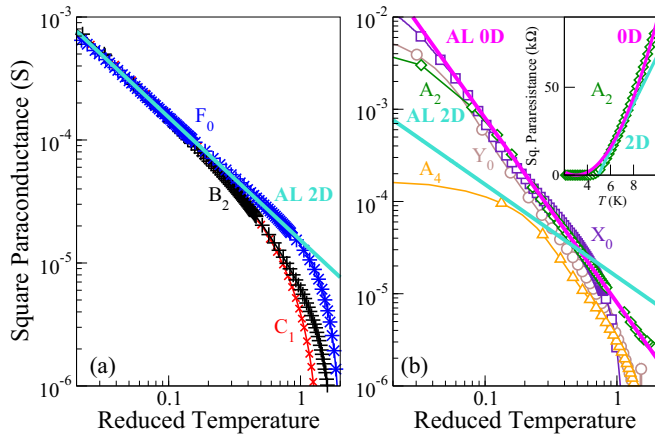


FIG. 4. (a) Extracted square paraconductance for the thicker samples B_2 ($T_c = 7.1$ K, pluses), C_1 ($T_c = 9.4$ K, crosses), and F_0 ($T_c = 9.0$ K, asterisks) as a function of the reduced temperature $\epsilon \equiv \ln(T/T_c)$. The agreement with the Aslamazov-Larkin prediction for a 2D system (blue solid line) is excellent, without any adjustable parameter. (b) Extracted square paraconductance for the thinner samples Y_0 ($T_c = 4.3$ K, open circles), X_0 ($T_c = 3.8$ K, open squares), A_2 ($T_c = 4.5$ K, open diamonds), and A_4 ($T_c = 2.4$ K, open triangles). The pink solid line corresponds to $\Delta\sigma = 0.03e^2/(\hbar\epsilon^2)$. The expected AL 2D square paraconductance is also shown (blue solid line). The inset shows the pararesistance $\Delta\sigma^{-1}$ as a function of temperature for the sample A_2 , emphasizing the 2D [$\propto (T - T_c)$] and 0D [$\propto (T - T_c)^2$] behaviors, the crossover from one to the other, and the different fluctuative critical temperatures in the two regimes ($T_c^{2D} = 4.9$ K, $T_c^{0D} = 4.4$ K). (See the Supplemental Material for more details about this crossover.)

Proceeding in a similar way, we extracted the paraconductivity of the thinner samples A_2, A_4 (aged A_2), X_0 , and Y_0 [shown as open symbols in Fig. 4(b)]. The AL 2D prediction is displayed in Fig. 4(b) (blue solid line). The experimental paraconductance is found to deviate strongly from the AL 2D behavior over a significant temperature range, even when using T_c as a free parameter. As a matter of fact, it is found to exhibit, *for all four samples and over a substantial range of reduced temperature*, a very specific law, $\Delta\sigma \sim \epsilon^{-2}$, corresponding to 0D fluctuations and previously observed in granular materials [35–38]. An empirical fitting function, $\Delta\sigma = 0.03e^2/(\hbar\epsilon^2)$, is plotted for comparison (pink solid line). The paraconductance data, e.g., for sample A_2 , also suggest a 0D-2D crossover [see the inset in Fig. 4(b)] as previously observed in [39] and discussed in [36]. Since the fluctuative critical temperature may differ in the two regimes, the crossover is better evidenced when the pararesistivity $\Delta\sigma^{-1}$ is plotted as a function of T , without making any choice for T_c , rather than ϵ , which depends on T_c . (This possible crossover is further discussed in the Supplemental Material.)

In order to show that the choice for T_c does not impact our findings, we plotted for sample A_2 the experimental paraconductance as a function of temperature for different values of T_c (see Fig. 5). It is clear in Fig. 5 that although the observation of the 2D regime may depend on the choice made for T_c , which is attributable to the fact that T_c^{2D} and T_c^{0D} are not necessarily equal as mentioned above, the 0D regime is

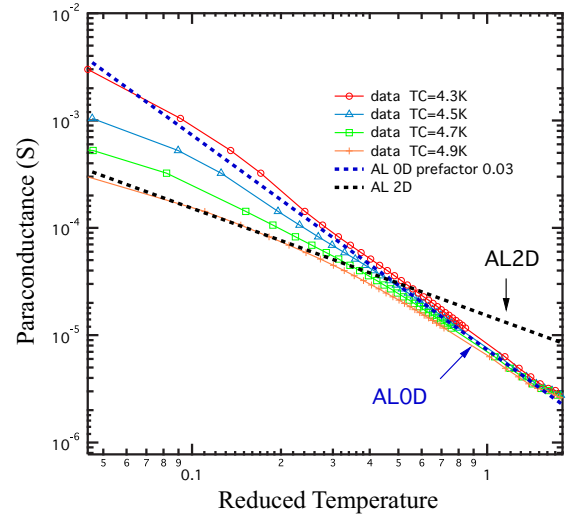


FIG. 5. Demonstration of the robustness of the 0D regime with respect to the choice of T_c . The experimental paraconductance is plotted for sample A_2 for different values of the critical temperature $T_c = 4.3$ K (red circles), $T_c = 4.5$ K (blue triangles), $T_c = 4.7$ K (green squares), and $T_c = 4.9$ K (orange crosses). The theoretical expectations for Aslamazov-Larkin fluctuations are also plotted: black dashed line for the 2D regime, no adjustable parameter, and blue dashed line for the 0D regime $\Delta\sigma = 0.03e^2/(\hbar\epsilon^2)$. One may see that, although the observation of the 2D regime may depend on the choice made for T_c , the 0D regime is always observed.

always observed and is extremely robust with respect to the choice for T_c .

C. Study of the magnetic-field-driven transition

The above study near T_c was complemented by the analysis of the transport properties of the thinnest samples at the transition to the normal state driven by magnetic field, well below T_c . We found that the curves $R(H)$ cross at a specific point, $\{R_C; H_C\}$ (see Fig. 3 of the Supplemental Material for the raw data). Following [40], we analyzed the curves in the vicinity of this point and found a scaling behavior of the type $R/R_C = f(|H - H_C|T^{-\alpha})$ with the critical exponent $\alpha \approx 3/2$ [see the data in Fig. 6(a) for sample A_2]. The occurrence of such a scaling behavior, where T is the only relevant scale, marks the existence of a quantum critical point (QCP) at zero temperature and for $H = H_C$. Consequently, the exponent α can be expressed as $\alpha = 1/(\nu z)$, where ν is the exponent that rules the variation of the spatial correlation length $\xi \sim |H - H_C|^{-\nu}$ and z is the dynamical critical exponent $\xi^z \sim 1/T$.

In order to extract the values of ν and z from $\alpha \approx 3/2$, similar measurements were performed at a fixed temperature, $T = 1.9$ K, for different values of the electric field, i.e., of the bias voltage across the sample [see the data for sample A_2 in Fig. 6(b)]. Here again, the $R(H)$ curves exhibit a common crossing point corresponding to the QCP (see Fig. 4 in the Supplemental Material). The scaling analysis in the vicinity of this point, with a scaling function of the form $R/R_C = g(|H - H_C|E^{-\beta})$, yielded $\beta \approx 3/4$. Following the analysis in [40–42], we express β as $\beta = 1/(\nu(z + 1))$. The two independent determinations of νz and $\nu(z + 1)$ allow us to establish

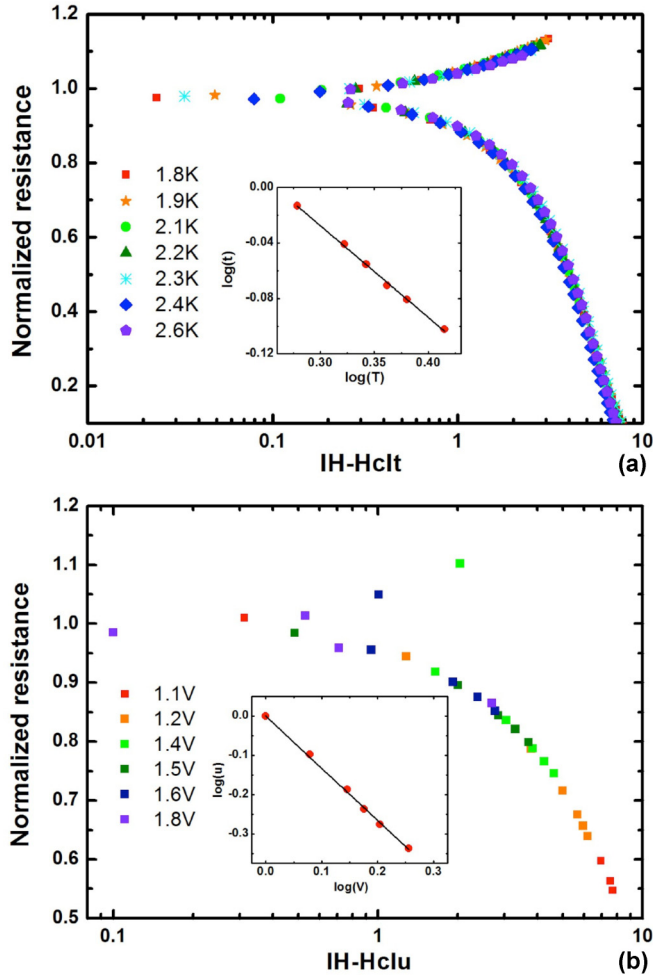


FIG. 6. (a) Normalized resistance R/R_C of sample A_2 as a function of the scaling variable $|H - H_C|t$ for different temperatures. $H_C = 10.7$ T and $R_C = 11$ k Ω at the crossing point. $t \equiv T^{-1/\nu z}$ was adjusted in order to obtain the best collapse of the data. Inset: Log-log plot of the parameter t vs temperature, used to determine the value of $\nu z = 2/3$. (b) Normalized resistance R/R_C of sample A_2 as a function of the scaling variable $|H - H_C|u$ for different electrical fields, measured at $T = 1.9$ K. $u \equiv E^{-1/\nu(z+1)}$ was adjusted in order to obtain the best collapse of the data. Inset: Log-log plot of the parameter u vs voltage used to determine the value of $\nu(z + 1) = 4/3$.

$\nu = 2/3$ and $z = 1$. The latter is precisely the result expected, e.g., in systems with (weakly screened) long-range Coulomb interactions, while the former is consistent with a 3D classical XY model or 2D quantum XY model (with $z = 1$). (A similar analysis, performed on sample F_0 under high pulsed magnetic field, allowed us to find a plateau between 1.5 and 8 K for $H_C = 18.6$ T and to extract a product of critical exponents $\nu z \sim 2/3$.)

III. DISCUSSION

A. Aslamazov-Larkin regime of fluctuations

The interplay between localization and fluctuation conductivity has been investigated from a theoretical point of view, and it has been shown that even close to the localization threshold, the transition remains narrow in temperature [43].

In particular theories have made a distinction between regimes of either weak or strong quantum fluctuations [44]. However, the observation of a conventional regime of fluctuation of the order parameter à la Aslamazov-Larkin [30] just above T_c is remarkable and surprising for two reasons apart from the already surprising zero-dimensional character of this regime. First, it seems at odds with the observation of a pseudogap, which is usually ascribed to the localization of Cooper pairs and should be accompanied by phase fluctuations with a well-defined amplitude for the order parameter [45]. Second, the fact that no correction to AL 2D is present in the vicinity of T_c for all the samples and in particular for the ones that exhibit a substantial range of 2D fluctuations, where the prefactor cannot be adjusted by tuning of a parameter, is surprising since MT [31,32] and DOS corrections are expected.

Concerning the absence of MT terms, one may stress that, with pair breaking arising only from electron-electron interactions, MT paraconductance is less singular than the AL term in 2D [46] and even less so for 0D AL, so it may be negligible close to T_c . On the other hand, the presence of a sizable pseudogap suggests that DOS corrections should be present. DOS corrections, however, are expected to lead to a decrease of the paraconductance. In our case, instead, the paraconductance in the pseudogap regime is found to be even more singular, with ϵ^{-2} dependence, which cannot be explained by DOS contribution. This clearly indicates that DOS corrections, although expected, are immaterial in this case.

As demonstrated in the Supplemental Material, the coherence-length exponent that leads to the observation of an anomalous power law $\Delta\sigma \sim \epsilon^{-2}$ is consistent with a formal calculation of AL fluctuations in a 0D system. $\Delta\sigma$ is converted into the measured paraconductance per square by means of the length scale l_{sg} , which represents the size of the 0D fluctuating domains, in the plane parallel to the film, yielding

$$\delta\sigma_{D=0} = \left(\frac{\xi_0}{l_{sg}}\right)^2 \frac{\pi e^2}{4\hbar\epsilon^2}. \quad (1)$$

Deducing for ξ_0 a value of 5.5 ± 0.5 nm from the value of H_C at the QCP, in agreement with extrapolated values in [26], it is possible to extract l_{sg} from the paraconductivity data. One finds, e.g., $l_{sg} = 28$ nm for samples A_2 ($T_c = 4.5$ K) and X_0 ($T_c = 3.8$ K), $l_{sg} = 35$ nm for sample Y_0 ($T_c = 4.3$ K), and $l_{sg} = 40$ nm for sample A_4 . This length l_{sg} is in quantitative agreement with the typical domain size $L_i/2 \sim 50$ nm extracted from STS data at 300 mK and at 4.2 K for sample X_0 ($T_c = 3.8$ K). This means that the length $L_i/2 \sim l_{sg}$ and not the real grain size $d_g \ll l_{sg}$ sets the scale for the 0D fluctuating domains until ξ becomes larger than L_i .

To our knowledge, the only previous evidence in the literature of a 0D fluctuation regime in transport is for nominally granular or filamentary systems [35,37,38]. The novelty lies here in the observation of such behavior in a compound where the inhomogeneity arises in a “mild” way: The films are far from granularity because the 0D behavior does not occur on the small scale of the crystallites, but rather on the larger typical scale l_{sg} , comparable to the correlation length $L_i/2$ inferred from STS. The emergent (as opposed to the structural) character of the 0D regions is also suggested

by the lack of any correlation [see Fig. 1(c)] between the inhomogeneous domains observed with STS [Fig. 1(b)] and the large-scale structural disorder observed in the topography of the crystallite ensemble [Fig. 1(a)]. The fact that these relatively smooth inhomogeneities give rise to a kind of confinement of the superconducting fluctuations leading to zero-dimensional behavior is indeed extremely surprising.

Finally, although we made a distinction here in the observed behavior of groups of thinner and thicker samples, we denote that thickness is certainly not the only parameter governing the distance to the transition. The major role is played by the particular disorder realization in the sample at both the nanoscopic and mesoscopic scales. Aging is definitely an issue, modifying substantially the realization of disorder. In addition, there is certainly no abrupt threshold between the thicker and thinner samples, and the distinction that we made was to stress two opposite tendencies. The reality seems more to be that the observable range for the 0D regime gradually shrinks when T_c is raised, progressively giving way to the 2D regime in the whole experimentally accessible range.

B. The 0D-2D crossover

For the superconducting transition to be probed in transport, the 0D fluctuation regime has to finally evolve to higher-dimensional behavior. Close enough to T_c a crossover to 2D behavior must (and does) occur when the superconducting coherence length becomes larger than L_i and enables us to couple different 0D domains, following a scenario analogous to the Lawrence-Doniach description for lamellar materials [36,47]. As a matter of fact, the 0D-2D crossover is visible for sample X_0 ($d = 2.14$ nm), as well as for sample A_2 ($d = 2.16$ nm). (See the inset of Figs. 4 and 5.)

However, we suggest here a different physical explanation for this crossover. We start with an expression of the AL paraconductivity in D dimensions [30,48–50] (see details in the Supplemental Material):

$$\delta\sigma_D(\epsilon) = \frac{\pi e^2}{4\hbar D} \int_0^\infty d\gamma \frac{\mathcal{N}_D(\gamma)}{(\epsilon + \gamma)^3}, \quad (2)$$

with a suitable “density of states” (weighted with current vertices) $\mathcal{N}_D(\gamma)$. Setting $D = 2$, the standard AL result is found for $\mathcal{N}_2(\gamma) = \gamma/\pi$, corresponding to diffusion of fluctuating Cooper pairs in two dimensions. However, if

$$\mathcal{N}_2(\gamma) = \begin{cases} \gamma/\pi & \text{for } \gamma \leq \bar{\gamma}, \\ \bar{\gamma}/\pi & \text{for } \gamma > \bar{\gamma}, \end{cases} \quad (3)$$

corresponding to a diffusion slowdown of fluctuating Cooper pairs above a threshold $\bar{\gamma}$, a 0D behavior

$$\delta\sigma \approx \frac{e^2 \bar{\gamma}}{16\hbar\epsilon^2} \quad (4)$$

is found for $\epsilon \gg \bar{\gamma}$. A comparison with the formal extrapolation of AL fluctuations to $D = 0$ yields $\bar{\gamma} = 4\pi(\xi_0/l_{sg})^2$. For $\epsilon \ll \bar{\gamma}$, the standard 2D AL paraconductivity is recovered.

The observed behavior could therefore be interpreted in terms of a diffusion slowdown of the Cooper pairs, thus increasing their lifetime on length scales smaller than l_{sg} . This might occur either because they locally find a more suitable environment, e.g., a locally stronger coupling, or, conversely,

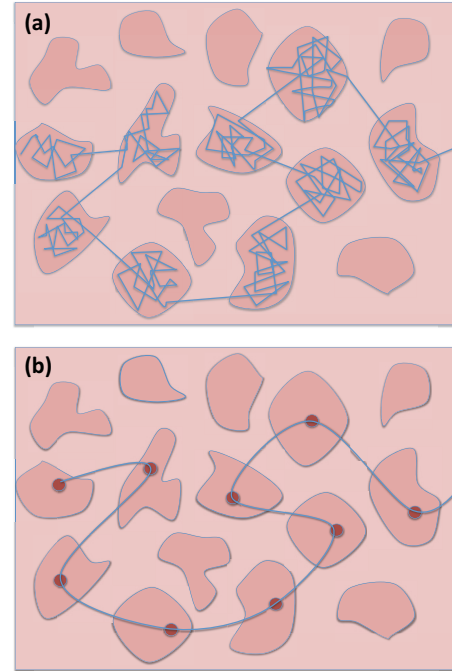


FIG. 7. Sketch of the anomalous diffusion of the Cooper modes induced by the emergent granularity in ultrathin NbN films. The supergrains are represented by the finite-size patches. In (a) the multiple scattering inside each supergrain depicts the diffusion slowdown leading to “confinement” of the fluctuating Cooper pairs, which gives way to the existence of a pseudogap and to the zero-dimensional character of the fluctuations. (b) Over longer distance and time scales a “coarse-grained” standard diffusive behavior of the Cooper pairs is recovered, leading to the usual 2D AL behavior.

because they display an increased tendency to localize for the wave vectors corresponding to the largest inhomogeneities. This second possibility seems more likely because our fits suggest that the 0D critical temperature (i.e., the “local” critical temperature) is slightly lower than the 2D large-scale T_c . By contrast, a standard diffusive behavior would be recovered at longer times and larger distances, giving way to standard 2D behavior eventually ruling the transition (see Fig. 7 and the Supplemental Material).

Finally, at even lower temperature (below the 2D AL transition temperature), the system might be governed by percolation physics or, alternately, by Berezinski-Kosterlitz-Thouless (BKT) behavior. This latter behavior, if present in our systems, should occur on a very restricted range of temperature because our measurements display the paraconductivity of conventional Gaussian fluctuations in the whole observation range.

It should be noted that a similar 0D-3D crossover has also been predicted by Lerner and coworkers [51] in a granular model in which the intragrain 0D paraconductivity is corrected by the Josephson tunneling probability between grains. The situation here is rather different since the DOS between the supergrains measured by STS is clearly not insulating; therefore the supergrains in which the 0D behavior is observed are not coupled by tunneling processes.

C. Nature of the pseudogap

In a regular “bosonic” scenario, the transition should be ruled by phase (and not amplitude) fluctuations of the order parameter, and the paraconductivity should mirror the characteristics of the vortex fluctuations in the BKT transition [45]. So, at first glance, our findings seem at odds with the existence of a pseudogap on the normal side of the transition that is well established in the literature and can be seen in the conductance maps and dI/dV spectra in Fig. 2(b) and that is usually ascribed to the localization of Cooper pairs [19,24]. Our work indeed suggests a different explanation for the pseudogap, and the experimental results reflect an intermediate situation in which the pairs are, in a certain sense, “confined” in a “supergrain” over the distance $l_{sg} \sim L_i/2$ without being strictly localized.

We propose, as described above, that the diffusion slowdown of the fluctuating Cooper pair in the supergrains increases their lifetime. This incipient diffusion slowdown of the Cooper pairs has a sizable effect on depressing the density of states at the Fermi level, which suggests the possibility of a substantial *fluctuational* pseudogap [25,33].

D. Transition under magnetic field

The magnetic-field-driven transition at low temperature can be interpreted as a magnetic-field-induced dephasing of the 0D supergrains, thereby accounting for the critical exponents $\nu = 2/3$ of an XY model in 2+1 dimensions, with the additional dimension coming from the dynamical critical index $z = 1$. The value $z = 1$ is pertinent, e.g., to systems with (weakly screened) long-range Coulomb interactions [52]. It is also consistent with numerical calculations based on a Bose-Hubbard model [53]. Similar values for ν were observed in Bi [42] or NbSi [54] amorphous thin films, whereas a large number of studies of the SIT point towards a different universality class with $\nu = 4/3$ [41,55–57], a critical exponent consistent with classical percolation. Our findings are therefore in agreement with a picture of phase-fluctuating 0D supergrains coupled à la Josephson for the magnetically driven transition. This may well be related to dynamic clustering of fluctuating Cooper pairs as proposed by [58].

E. Origin of the inhomogeneities

The question arises of the origin of the superconducting inhomogeneities. Indeed, while the structural small-scale inhomogeneity associated with the structural grains (2–5 nm) appears to be irrelevant, we deal with three larger scales over distances of tens of nanometers: (a) the electronic inhomogeneity of the pseudogap seen by STS [Fig. 1(b); $L_i \approx 100$ nm], (b) the scale of the 0D AL behavior seen in transport ($l_{sg} \sim 50$ nm), and (c) the topographic smooth landscape [Fig. 1(a)]. Although scale (b) is obtained from transport and cannot easily be connected to a spatial structure, it is quite natural to associate the electronic scales of pseudogap and 0D transport $l_{sg} \sim L_i/2$ to the scale on which Cooper pairs tend to localize (before they eventually condense on the infinite scale of the 2D transition).

On the other hand, the fact that there is no correlation between the topographical map and the superconducting gap

map proves that the structure is not responsible for the gap inhomogeneities in a trivial way. That is, it is not some local parameter variation such as thickness that induces a locally correlated variation of the superconducting properties. This does not mean that disorder or structural inhomogeneities are irrelevant. They are most likely relevant, but in a complex manner; for instance, disorder is relevant for localization, but localization length is not simply the distance between impurities.

The variation of T_c and of the normal-state resistance with the nominal thickness is rather steep, which is an indication that thickness alone is not responsible for the T_c decrease. Aging of the samples is also shown to decrease T_c and increase R_{300K} , which indicates that structural and compositional effects most certainly come into play, increasing local disorder.

One is therefore tempted to raise the possibility that the films may suffer from compositional inhomogeneities, possibly giving rise to the superconducting inhomogeneities. This is, of course, highly possible. But one then still needs to explain why such smooth compositional inhomogeneities that are not visible on the topographic map (at least not on a scale in correlation to the supergrains) lead to such abrupt zero-dimensional confinement of superconducting fluctuations, while, on the contrary, the grain height variations seem to have little effect on the superconducting gap. On the other hand, even if these incipient inhomogeneities were to emerge in a spontaneous manner, the supergrains should have a tendency to pin onto the less disordered regions. This spontaneous (or not) character is therefore very difficult to decipher.

In any case, the main result of our work is that a 0D physics is found to emerge in transport measurements on the same length scale as the length scale for the superconducting inhomogeneities, much larger than the structural crystallites, indicating that the structural complexity has an electronic counterpart producing some anomalous diffusion (and a possible slowing down) of the Cooper pairs. Further investigation is needed to understand how the proposed anomalous diffusion processes emerge from a given disorder realization.

IV. CONCLUSION

The emergence of (glassy) inhomogeneous superconducting phases out of homogeneously disordered films has been proposed theoretically [12,16,20] and measured experimentally [19,22,23]. Our STS measurements have evidenced electronic inhomogeneities with a typical correlation length ($L_i \approx 100$ nm) and typical domain size $L_i/2$ in the superconducting state below T_c and in the superconducting fluctuations above T_c in NbN ultrathin films. These inhomogeneities, which are much larger than the structural grains of the film made of nanometer-sized nanocrystals, correspond to simultaneous spatial variations of the energy of the superconducting gap and of the energy-integrated in-gap conductance and are found to become dominating for the thinner samples, in which they strongly affect the superconductive thermal fluctuations. Specifically, we have shown that, for films with nominal thickness $d < 2.3$ nm or $T_c < 0.3 T_c^{\text{bulk}}$, these inhomogeneities are associated with specific exponents in the dependence of the Gaussian superconducting fluctuations on reduced temperature. These exponents are consistent with AL fluctuations

confined to 0D supergrains of size $l_{sg} \sim L_i/2$. On the other hand, at low temperature, the analysis of the magnetic-field-driven transition is consistent with a 2D quantum XY model, which is evocative of 0D supergrains coupled à la Josephson. In this regime, the Cooper pairs are tightly bound, and the transition is ruled by supergrain dephasing, in contrast to the transition at finite temperature, where AL *amplitude fluctuations* are instead observed.

We propose that, above T_c , diffusion slowing down the Cooper pairs in the supergrains increases their lifetime and leads to a depression in the density of states at the Fermi level, yielding a fluctuational pseudogap. The origin of these inhomogeneities as well as these anomalous diffusion processes still needs to be investigated.

In any case, this work argues for a new theoretical microscopic description of this peculiar state of matter, with the interplay of anomalous diffusion and pairing, where Cooper

pairs are confined over l_{sg} but not localized in a strict sense, and pictures an intermediate situation somewhere in between the Fermi and Bose insulator paradigms.

ACKNOWLEDGMENTS

This work has been supported by a SESAME grant from Region Ile-de-France. Collaboration with Università di Roma La Sapienza was supported by CNRS through a PICS program (S2S) and by a Joliot grant from ESPCI Paris. The work at INSP was supported by the Emergence-UPMC program. We acknowledge the support of the LNCMI-CNRS, a member of the European Magnetic Field Laboratory (EMFL), and EMFL support for Contract No. TMF07-114. The work at INSP and Karlsruhe was supported by the Superstripes grant from the French-German ANR-DFG bilateral funding program, under the Project No. ANR-15-CE30-0026-02.

[1] G. N. Gol'tsman *et al.*, Picosecond superconducting single-photon optical detector, *Appl. Phys. Lett.* **79**, 705 (2001).

[2] M. Hofherr, D. Rall, K. Ilin, M. Siegel, A. Semenov, H. W. Hübers, and N. A. Gippius, Intrinsic detection efficiency of superconducting nanowire single-photon detectors with different thicknesses, *J. Appl. Phys.* **108**, 014507 (2010).

[3] A. M. Goldman and N. Marković, Superconductor-insulator transitions in the two-dimensional limit, *Phys. Today* **51**(11), 39 (1998).

[4] I. Beloborodov, A. Lopatin, V. Vinokur, and K. Efetov, Granular electronic systems, *Rev. Mod. Phys.* **79**, 469 (2007).

[5] A. M. Finkel'shtein, Superconductivity-transition temperature in amorphous films, *Pis'ma Zh. Eksp. Teor. Fiz.* **45**, 37 (1987) [*JETP Lett.* **45**, 46 (1987)].

[6] J. M. Valles, Jr., R. C. Dynes, and J. R. Garno, Electron Tunneling Determination of the Order-Parameter Amplitude at the Superconductor-Insulator Transition in 2D, *Phys. Rev. Lett.* **69**, 3567 (1992).

[7] M. P. A. Fisher, G. Grinstein, and S. M. Girvin, Presence of Quantum Diffusion in Two Dimensions: Universal Resistance at the Superconductor-Insulator Transition, *Phys. Rev. Lett.* **64**, 587 (1990).

[8] M. P. A. Fisher, Quantum Phase Transitions in Disordered Two-Dimensional Superconductors, *Phys. Rev. Lett.* **65**, 923 (1990).

[9] G. Seibold, L. Benfatto, C. Castellani, and J. Lorenzana, Superfluid Density and Phase Relaxation in Superconductors with Strong Disorder, *Phys. Rev. Lett.* **108**, 207004 (2012).

[10] M. Feigel'man, L. Ioffe, V. Kravtsov, and E. Yuzbashyan, Eigenfunction Fractality and Pseudogap State near the Superconductor-Insulator Transition, *Phys. Rev. Lett.* **98**, 027001 (2007).

[11] M. V. Feigel'man, L. B. Ioffe, V. E. Kravtsov, and E. Cuevas, *Ann. Phys. (N.Y.)* **325**, 1390 (2010).

[12] L. B. Ioffe and M. Mézard, Disorder-Driven Quantum Phase Transitions in Superconductors and Magnets, *Phys. Rev. Lett.* **105**, 037001 (2010).

[13] S. M. Hollen, G. E. Fernandes, J. M. Xu, and J. M. Vallès, Collapse of the Cooper pair phase coherence length at a superconductor-to-insulator transition, *Phys. Rev. B* **87**, 054512 (2013).

[14] M. D. Stewart, A. Yin, J. M. Xu, and J. M. Valles, Superconducting pair correlations in an amorphous insulating nanohoneycomb film, *Science* **318**, 1273 (2007).

[15] G. Kopnov, O. Cohen, M. Ovadia, K. Hong Lee, C. C. Wong, and D. Shahar, Little-Parks Oscillations in an Insulator, *Phys. Rev. Lett.* **109**, 167002 (2012).

[16] G. Lemarié, A. Kamlapure, D. Bucheli, L. Benfatto, J. Lorenzana, G. Seibold, S. C. Ganguli, P. Raychaudhuri, and C. Castellani, Universal scaling of the order-parameter distribution in strongly disordered superconductors, *Phys. Rev. B* **87**, 184509 (2013).

[17] M. V. Feigel'man, and M. A. Skvortsov, Universal Broadening of the Bardeen-Cooper-Schrieffer Coherence Peak of Disordered Superconducting Films, *Phys. Rev. Lett.* **109**, 147002 (2012).

[18] B. Sacépé, C. Chapelier, T. I. Baturina, V. M. Vinokur, M. R. Baklanov, and M. Sanquer, Disorder-Induced Inhomogeneities of the Superconducting State Close to the Superconductor-Insulator Transition, *Phys. Rev. Lett.* **101**, 157006 (2008).

[19] B. Sacépé, T. Dubouchet, C. Chapelier, M. Sanquer, M. Ovadia, D. Shahar, M. Feigel'man, and L. Ioffe, Localization of preformed Cooper pairs in disordered superconductors, *Nat. Phys.* **7**, 239 (2011).

[20] K. Bouadim, Y. L. Loh, M. Randeria, and N. Trivedi, Single- and two-particle energy gaps across the disorder-driven superconductor-insulator transition, *Nat. Phys.* **7**, 884 (2011).

[21] N. Trivedi, Y. L. Loh, K. Bouadim, and M. Randeria, Emergent granularity and pseudogap near the superconductor-insulator transition, *J. Phys.: Conf. Ser.* **376**, 012001 (2012).

[22] A. Kamlapure, T. Das, S. C. Ganguli, J. B. Parmar, S. Bhattacharyya, and P. Raychaudhuri, Emergence of nanoscale inhomogeneity in the superconducting state of a homogeneously disordered conventional superconductor, *Sci. Rep.* **3**, 2979 (2013).

[23] Y. Noat *et al.*, Unconventional superconductivity in ultrathin superconducting NbN films studied by scanning tunneling spectroscopy, *Phys. Rev. B* **88**, 014503 (2013).

[24] B. Sacépé, C. Chapelier, T. I. Baturina, V. M. Vinokur, M. R. Baklanov, and M. Sanquer, Pseudogap in a thin film of a conventional superconductor, *Nat. Commun.* **1**, 140 (2010).

- [25] E. Abrahams, M. Redi, and J. Woo, Effect of fluctuations on electronic properties above the superconducting transition, *Phys. Rev. B* **1**, 208 (1970).
- [26] A. Semenov *et al.*, Optical and transport properties of ultrathin NbN films and nanostructures, *Phys. Rev. B* **80**, 054510 (2009).
- [27] See Supplemental Material at <http://link.aps.org/supplemental/10.1103/PhysRevB.93.144509> for details about sample fabrication and characterization, measurement methods, additional data and parameters and theoretical calculation of the paraconductivity.
- [28] B. L. Altshuler, A. G. Aronov, and P. A. Lee, Interaction Effects in Disordered Fermi Systems in Two Dimensions, *Phys. Rev. Lett.* **44**, 1288 (1980).
- [29] C. Carbillet *et al.* (unpublished).
- [30] L. G. Aslamasov and A. I. Larkin, The influence of fluctuation pairing of electrons on the conductivity of normal metal, *Phys. Lett. A* **26**, 238 (1968).
- [31] K. Maki, Critical fluctuation of the order parameter in a superconductor. I, *Prog. Theor. Phys.* **40**, 193 (1968).
- [32] R. S. Thompson, Microwave, flux flow, and fluctuation resistance of dirty type-II superconductors, *Phys. Rev. B* **1**, 327 (1970).
- [33] I. S. Beloborodov and K. B. Efetov, Negative Magnetoresistance of Granular Metals in a Strong Magnetic Field, *Phys. Rev. Lett.* **82**, 3332 (1999).
- [34] I. S. Beloborodov, K. B. Efetov, and A. I. Larkin, Magnetoresistance of granular superconducting metals in a strong magnetic field, *Phys. Rev. B* **61**, 9145 (2000).
- [35] J. Kirtley, Y. Imry, and P. K. Hansma, Fluctuation-induced conductivity above the critical temperature in small-particle arrays, *J. Low Temp. Phys.* **17**, 247 (1974).
- [36] G. Deutscher, Y. Imry, and L. Gunther, Superconducting phase transitions in granular systems, *Phys. Rev. B* **10**, 4598 (1974).
- [37] R. I. Civiak, C. Elbaum, L. F. Nichols, H. I. Kao, and M. M. Labes, Fluctuation-induced conductivity and dimensionality in polysulfur nitride, *Phys. Rev. B* **14**, 5413 (1976).
- [38] S. Wolf and W. H. Lowrey, Zero Dimensionality and Josephson Coupling in Granular Niobium Nitride, *Phys. Rev. Lett.* **39**, 1038 (1977).
- [39] B. I. Belevstsev and Yu F. Komnik, Superconducting fluctuations above T_c in cold-deposited indium films with hydrogen: Observation of transition from two to zero dimensional fluctuations, *Sov. J. Low Temp. Phys.* **9**, 3 (1983).
- [40] S. L. Sondhi, S. M. Girvin, J. P. Carini, and D. Shahar, Continuous quantum phase transitions, *Rev. Mod. Phys.* **69**, 315 (1997).
- [41] A. Yazdani and A. Kapitulnik, Superconducting-Insulating Transition in Two-Dimensional α -MoGe Thin Films, *Phys. Rev. Lett.* **74**, 3037 (1995).
- [42] N. Marković, C. Christiansen, A. M. Mack, W. H. Huber, and A. M. Goldman, Superconductor-insulator transition in two dimensions, *Phys. Rev. B* **60**, 4320 (1999).
- [43] L. N. Bulaevskii, A. A. Varlamov, and M. V. Sadovskii, Fluctuations of the conductivity and diamagnetic susceptibility in dirty superconductors near the Anderson localization threshold, *Sov. Phys. Solid State* **28**, 997 (1986).
- [44] A. Larkin, Superconductor-insulator transitions in films and bulk materials, *Ann. Phys. (Berlin, Ger.)* **8**, 785 (1999).
- [45] B. I. Halperin and D. R. Nelson, Resistive Transition in Superconducting Films, *J. Low Temp. Phys.* **36**, 599 (1979).
- [46] M. Y. Reizer, Fluctuation conductivity above the superconducting transition: Regularization of the Maki-Thompson term, *Phys. Rev. B* **45**, 12949 (1992).
- [47] W. E. Lawrence and S. Doniach, in *Proceedings of the Twelfth International Conference on Low Temperature Physics*, edited by E. Kanda (Academic Press of Japan, Kyoto, 1971), p. 361.
- [48] S. Caprara, M. Grilli, B. Leridon, and J. Lesueur, Extended paraconductivity regime in underdoped cuprates, *Phys. Rev. B* **72**, 104509 (2005).
- [49] S. Caprara, M. Grilli, B. Leridon, and J. Vanacken, Paraconductivity in layered cuprates behaves as if due to pairing of nearly free quasiparticles, *Phys. Rev. B* **79**, 024506 (2009).
- [50] B. Leridon, J. Vanacken, T. Wambecq, and V. V. Moshchalkov, Paraconductivity of underdoped $\text{La}_{2-x}\text{Sr}_x\text{CuO}_4$ thin-film superconductors using high magnetic fields, *Phys. Rev. B* **76**, 012503 (2007).
- [51] I. V. Lerner, A. A. Varlamov, and V. M. Vinokur, Fluctuation Spectroscopy of Granularity in Superconducting Structures, *Phys. Rev. Lett.* **100**, 117003 (2008).
- [52] I. Herbut, Quantum Critical Points with the Coulomb Interaction and the Dynamical Exponent: When and Why $z = 1$, *Phys. Rev. Lett.* **87**, 137004 (2001).
- [53] J. Kisker and H. Rieger, Bose-glass and Mott-insulator phase in the disordered boson Hubbard model, *Phys. Rev. B* **55**, R11981 (1997).
- [54] H. Aubin, C. A. Marrache-Kikuchi, A. Pourret, K. Behnia, L. Bergé, L. Dumoulin, and J. Lesueur, Magnetic-field-induced quantum superconductor-insulator transition in $\text{Nb}_{0.15}\text{Si}_{0.85}$, *Phys. Rev. B* **73**, 094521 (2006).
- [55] A. F. Hebard and M. A. Paalanen, Magnetic-Field-Tuned Superconductor-Insulator Transition in Two-Dimensional Films, *Phys. Rev. Lett.* **65**, 927 (1990).
- [56] A. Kapitulnik, N. Mason, S. Kivelson, and S. Chakravarty, Effects of dissipation on quantum phase transitions, *Phys. Rev. B* **63**, 125322 (2001).
- [57] M. Steiner and A. Kapitulnik, Superconductivity in the insulating phase above the field-tuned superconductor-insulator transition in disordered indium oxide films, *Phys. C (Amsterdam, Neth.)* **422**, 16 (2005).
- [58] A. Glatz, A. A. Varlamov, and V. M. Vinokur, Quantum fluctuations and dynamic clustering of fluctuating Cooper pairs, *Europhys. Lett.* **94**, 47005 (2011).